Neutral and Ionic Metal-Hydrogen and Metal-Carbon Bond Energies: Reactions of Co^+, Ni^+, and Cu^+ with Ethane, Propane, Methylpropane, and Dimethylpropane

R. Georgiadis,[†] Ellen R. Fisher,[‡] and P. B. Armentrout*[,‡,§]

Contribution from the Department of Chemistry, University of California, Berkeley, California 94720, and Department of Chemistry, University of Utah, Salt Lake City, Utah 84112. *Received December 27, 1988*

Abstract: The reactions of Co^+, Ni^+, and Cu^+ with a series of alkanes are examined by guided ion beam mass spectrometry. The emphasis of this study is on C-H and C-C bond cleavage channels from which bond dissociation energies for M-H, M-CH_3, and M^+-CH_3 are derived from the endothermic reaction thresholds. For these three bond energies, we find values (in kilocalories per mole) of 46 ± 3, 46 ± 3, and 49.1 ± 3.5, respectively, for M = Co; 58 ± 3, 55 ± 3, and 45.0 ± 2.4, respectively, for M = Ni; 61 ± 4, 58 ± 2, 29.7 ± 1.7, respectively, for M = Cu. Trends in the thermochemistry of these species and M^+-H are briefly discussed. The reactivity of Cu^+, which has not been previously studied, is compared with that for other transition-metal ions. Also, unusual features in the reactivity of Co^+ and Ni^+ that have not previously been commented on are discussed.

The relative strength of M-H and M-CH_3 bonds is crucial to characterizing and understanding many organometallic reactions. Where measurements are available, M-H bonds are found to be substantially stronger than M-CH_3 bonds in condensed phase coordinately saturated transition-metal systems.[1] For unsaturated metal ion systems, however, the converse is true.[2] If the growing body of specific metal ligand bond energies determined in gas-phase studies is to be useful to the practicing organometallic chemist, such striking differences in condensed-phase and gas-phase thermochemical data must be understood. Proposed explanations for this difference between the condensed-phase and gas-phase bond strengths include steric weakening of the metal-alkyl bond in the saturated systems[3] and charge stabilization of the metal ion by the more polarizable alkyl group in the ionic species.[4,5] This latter hypothesis can be tested by comparing the bond energies for neutral vs ionic unsaturated metal-hydrides and metal-alkyls.

Bond energies for ionic transition-metal species have been obtained by ion beam mass spectrometry,[6] ion cyclotron resonance (ICR),[7] Fourier transform (FTMS),[8] and photoionization mass spectrometries.[9] Neutral metal hydride bond energies have been measured by spectroscopy,[10] high-temperature mass spectrometry,[11] and via bracketing measurements made with ion beams[12] and FTMS.[13] Recent work in our laboratory has demonstrated that guided ion beam mass spectrometry can yield reliable neutral and ionic bond dissociation energies for diatomic and polyatomic species.[2,14,15] This paper presents a continuation of these studies with an emphasis on the thermochemistry of ionic and neutral metal-methyl and metal-hydride bond energies. These can be measured by studies of the following four endothermic reactions:

$$M^+ + RCH_3 \rightarrow MCH_3^+ + R \quad (1)$$

$$M^+ + RH \rightarrow MH^+ + R \quad (2)$$

$$M^+ + RCH_3 \rightarrow MCH_3 + R^+ \quad (3)$$

$$M^+ + RH \rightarrow MH + R^+ \quad (4)$$

where R = CH_3, C_2H_5, 2-C_3H_7, t-C_4H_9. Only in the case of the metal-hydride *ion* bond energies are there more reliable values available. These come from previous studies of reaction 5 and its isotopic analogues.[16]

$$M^+ + H_2 \rightarrow MH^+ + H \quad (5)$$

The metals of interest in this paper are Co, Ni, and Cu. While no ion beam studies of Cu^+ with alkanes have been reported previously, the reactions of alkanes with Co^+ and Ni^+ have been studied with ion beam techniques by Armentrout and Beauchamp (AB)[4] and by Halle, Armentrout, and Beauchamp (HAB),[17] respectively. Along with the ICR studies of Allison and Ridge,[7] this work provided some of the first values for ionic and neutral metal-methyl and metal-hydride bond energies. Comprehensive beam[18,19] and FTMS[20] experiments have since sought to elucidate the mechanisms for reaction of Co^+ and Ni^+ with alkanes.

Here, we reexamine and reanalyze the reactions of Co^+ and Ni^+ with a series of saturated alkanes and present new results for the reactions of Cu^+. The emphasis of the present work is to provide new thermochemical values for $CuCH_3^+$ and the neutral

[†] University of California.
[‡] University of Utah.
[§] NSF Presidential Young Investigator, 1984-1989. Alfred P. Sloan Fellow. Camille and Henry Dreyfus Teacher-Scholar, 1987-1992.

(1) Halpern, J. *Acc. Chem. Res.* **1982**, *15*, 238-244; *Inorg. Chim. Acta* **1985**, *100*, 41-48.
(2) Armentrout, P. B.; Georgiadis, R. *Polyhedron* **1988**, *7*, 1573-1581.
(3) Ng, F. T. T.; Rempel, G. L.; Halpern, J. *Inorg. Chim. Acta* **1983**, *77*, L165.
(4) Armentrout, P. B.; Beauchamp, J. L. *J. Am. Chem. Soc.* **1981**, *103*, 784-791.
(5) Mandich, M. L.; Halle, L. F.; Beauchamp, J. L. *J. Am. Chem. Soc.* **1984**, *106*, 4403-4411.
(6) Armentrout, P. B.; Beauchamp, J. L. *J. Am. Chem. Soc.* **1980**, *102*, 1736; Armentrout, P. B.; Beauchamp, J. L. *J. Chem. Phys.* **1981**, *74*, 2819-2826.
(7) Allison, J.; Ridge, D. P. *J. Organomet. Chem.* **1975**, *99*, C11-C14. *J. Am. Chem. Soc.* **1976**, *98*, 7445-7447; **1979**, *101*, 4998-5009.
(8) Hettich, R. L.; Jackson, T. C.; Stanko, E. M.; Freiser, B. S. *J. Am. Chem. Soc.* **1986**, *108*, 5086-5093.
(9) Distefano, G.; Dibeler, V. H. *Int. J. Mass Spectrom. Ion Phys.* **1970**, *4*, 59.
(10) Huber, K. P.; Herzberg, G. *Molecular Spectra and Molecular Structure IV, Constants of Diatomic Molecules*; Van Nostrand Reinhold: New York, 1979.
(11) Kant, A.; Moon, K. A. *High Temp. Sci.* **1981**, *14*, 23; **1979**, *11*, 55.
(12) Tolbert, M. A.; Beauchamp, J. L. *J. Phys. Chem.* **1986**, *90*, 5015-5022.
(13) Sallans, L.; Lane, K. R.; Squires, R. R.; Freiser, B. S. *J. Am. Chem. Soc.* **1985**, *107*, 4379-4385. Squires, R. R. *Ibid.* **1985**, *107*, 4385-4390.
(14) (a) Georgiadis, R.; Armentrout, P. B. *J. Am. Chem. Soc.* **1986**, *108*, 2119-2126. (b) Boo, B. H.; Armentrout, P. B. *J. Am. Chem. Soc.* **1987**, *109*, 3459-3559. (c) Weber, M. E.; Armentrout, P. B. *J. Chem. Phys.* **1988**, *88*, 6898-6910.
(15) Schultz, R. H.; Elkind, J. L.; Armentrout, P. B. *J. Am. Chem. Soc.* **1988**, *110*, 411-423.
(16) Elkind, J. L.; Armentrout, P. B. *J. Phys. Chem.* **1986**, *90*, 6576-6586.
(17) Halle, L. F.; Armentrout, P. B.; Beauchamp, J. L. *Organometallics* **1982**, *1*, 963-968.
(18) Houriet, R.; Halle, L. F.; Beauchamp, J. L. *Organometallics* **1983**, *2*, 1818-1829.
(19) Hanratty, M. A.; Beauchamp, J. L.; Illies, A. J.; Koppen, P.; Bowers, M. T. *J. Am. Chem. Soc.* **1988**, *110*, 1-14.
(20) (a) Jacobson, D. B.; Freiser, B. S. *J. Am. Chem. Soc.* **1983**, *105*, 736-742; (b) *J. Am. Chem. Soc.* **1983**, *105*, 5197-5206.

0002-7863/89/1511-4251$01.50/0

species MH and MCH_3 where M = Co, Ni, and Cu. In the course of these studies, we also refine the bond energy previously measured for $NiCH_3^+$ and substantially alter that for $CoCH_3^+$. Further, the reactivity of Cu^+ is compared with that for the better studied Co^+ and Ni^+ systems, and unusual features in the latter two systems that have gone unnoticed are discussed.

Experimental Section

General Procedures. Experiments are performed on a guided ion beam apparatus, a detailed description of which has been given elsewhere.[21] Ions are extracted from the surface ionization source (see below) and then mass analyzed. The mass selected ion beam is decelerated to the desired kinetic energy and focused into an octopole ion trap, which passes through a gas cell containing a reactant gas. Single-collision conditions are maintained by operating at low pressures. Collection of all ionic products as well as transmitted reactant ions is maximized by the octopole guide which uses radio frequency electric fields to trap ions in the radial direction. Raw intensities of mass analyzed product ions and unreacted beam are converted to absolute cross sections as described previously.[21] The uncertainty in the absolute magnitude of the cross sections is estimated to be ±20%.

For the alkyl ion product cross sections, the uncertainty may be higher. For a given alkane system, the overall shape of the cross sections for the alkyl ion products can vary at higher energies. One reason for this is that alkyl ions are generally more difficult to collect efficiently because they may not be preferentially forward-scattered in the laboratory. Conditions were optimized for good collection in these experiments.

The absolute energy scale and ion energy distribution are determined by using the octopole as a retarding field analyzer to sweep through the nominal ion energy zero. The derivative of the resulting retarding curve is nearly Gaussian with a peak taken to be the energy scale zero and a width characteristic of the ion beam spread. The absolute uncertainty in the laboratory energy scale is ±0.05 eV. The laboratory ion energy is converted to center of mass energy by the equation, $E(CM) = E(lab) \times m/(M + m)$ where m and M are the mass of the neutral and ionic reactants, respectively. Thus, the energy scale uncertainty is <0.03 eV in the center of mass frame for all reactions studied here. There are two sources of energy broadening in these experiments: the ion beam kinetic energy distribution, which has a typical fwhm of ~0.5 eV (lab), and the thermal broadening due to motion of the neutral gas (so-called Doppler broadening).[21] In the reactions studied here, this effect has a fwhm ranging from 0.45- to $0.69E^{1/2}$ eV in the center of mass frame.

Ion Source. For these experiments, the ions $^{59}Co^+$ (100% natural abundance), $^{58}Ni^+$ (67.8% natural abundance), and $^{63}Cu^+$ (69.1% natural abundance) are produced in a surface ionization source described elsewhere.[16] For the reaction with isobutane and neopentane, $^{60}Ni^+$ (26.2% natural abundance) was used to reduce mass overlap between the reactant beam and one of the product ions (m/z 57, $C_4H_9^+$). Here, we use $CoCl_2$, $NiCl_2$, and $CuBr_2$ as metal sources and a rhenium filament temperature of 2200 ± 100 K. As discussed in detail elsewhere,[22] we presume that the ions equilibrate at this temperature, such that the source produces essentially pure ground-state $Ni^+(^2D)$ and $Cu^+(^1S)$ beams, 99.0% and >99.9%, respectively. The Co^+ beam contains only 85% of the ground-state $Co^+(^3F)$, with a significant quantity of excited-state ^5F (15%). However, from previous work,[16] we expect that $Co^+(^5F)$ will be relatively unreactive with alkanes. The effect of an unreactive component in the beam is simply to decrease the magnitude of the reaction cross sections.

Thermochemical Analysis. Exothermic reaction cross sections are usually described by the Langevin–Gioumousis–Stevenson (LGS) form[23]

$$\sigma_{LGS} = \pi q(2\alpha/E)^{1/2} \quad (6)$$

where q is the unit of electric charge, α is the polarizability of the neutral molecule, and E is the relative translational energy of the reactants. While this form of the cross section describes the energy dependence of many exothermic reaction cross sections, deviations from this behavior are common.[24]

To obtain quantitative thermochemistry, we analyze the threshold behavior of endothermic reactions to determine the reaction endothermicity. A general empirical trial function, which has been used to model endothermic reaction thresholds, is given in eq 7, where E is the relative

$$\sigma(E) = \sigma_0(E - E_T)^n/E^m \quad (7)$$

kinetic energy in the center of mass frame, E_T is the effective reaction threshold, σ_0 is a scaling factor, and n and m are adjustable parameters. The relationship between the effective threshold and the true threshold is given by eq 8, where E_{el} is the electronic energy of the metal ion

$$E_0 = E_T + E_{el} \quad (8)$$

reactant. For a filament temperature of 2200 K, the average electronic energy is 0.046 eV for $Co^+(^3F)$, 0.037 eV for $Ni^+(^2D)$, and 0.0 eV for $Cu^+(^1S)$.[16,25] The thermochemistry derived here is assumed to be at 298 K, the nominal temperature of the neutral reactant. For this reason, no corrections to the effective threshold are made for the internal energy of the neutral reactants.

A number of specific forms of eq 7 have been proposed, including one specifically for translationally driven reactions, in which m is equal to 1.0.[26] The method of analysis used here is a more flexible semiempirical form, in which n, σ_0, and E_T are allowed to vary while m is set to 1.0. To fit the data, eq 7 is convoluted with the experimental energy distributions before comparison with the data, as described in detail in previous work.[21]

Equation 7 was also evaluated for the cases where m = 0, 3, and n. The final determination of the endothermicity for a given reaction is the average value of E_T from these four fits to the data. We find that this average E_T agrees very well with the result of the m = 1 fit. We report only the parameters used in the m = 1 fits, including the analysis at high energies described below, and the uncertainties in these values. The error limits for E_T are calculated from the range of values for different fitting parameters, the deviations of the threshold values for different data sets, and the error in the absolute energy scale.

High-Energy Behavior. Endothermic reaction cross sections generally decline at higher translational energies due to dissociation of the product ion. Often, this occurs at the thermodynamic threshold for process 9,

$$M^+ + ABC \rightarrow MA^+ + BC \rightarrow M^+ + A + BC \quad (9)$$

$D°(A–BC)$. The peak of the cross section can be shifted to higher energies if energy goes selectively into translational energy or internal modes of the BC product. Similar considerations hold for products that do not contain the metal, such as those of reaction 10. Dissociation of

$$M^+ + ABC \rightarrow BC^+ + MA \rightarrow B^+ + C + MA \quad (10)$$

BC^+ can begin at $D°(A–BC) + D°(B–C) - D°(M–A) - IP(M) + IP(B)$, where IP(X) is the ionization potential of X.

The high-energy behavior has been described by using a model that is based on simple statistical assumptions about the probability of dissociation of the product, while conserving angular momentum.[27] There are two parameters in the high-energy modeling, E_D, which is the energy at which product dissociation begins, and p, which can be related to the number of degrees of freedom in the transition state. For the systems considered here, p is simply an empirical parameter that reflects the rate at which the cross section falls off. E_D is determined by the thermodynamics of reaction 9 or 10.

Results

Co^+, Ni^+, and Cu^+ react with alkanes to form a variety of products. The major products are remarkably similar for all three ions, although there are some notable differences. For example, Cu^+ does not react exothermically with alkanes as do Co^+ and Ni^+. Results for the latter two systems are in reasonable agreement with ion beam results previously obtained for Co^+ by Armentrout and Beauchamp (AB)[4] and Halle, Armentrout, and Beauchamp (HAB).[17] Reaction 2, formation of MH^+, is observed for all ions, although data were not collected for Cu^+. The reactivities of the three metal ions with each alkane are discussed below.

Ethane. Figure 1 shows the products for the reaction with ethane for Co^+, Ni^+, and Cu^+. The major products are MCH_3^+, MH^+, and $C_2H_5^+$, the ionic products of reactions 1, 2, and 4, respectively. Cu^+ shows reactivity very similar to that of the other ostensibly more reactive ions. Reaction 3, formation of CH_3^+, is not observed for any of the metal ions studied here. This is presumably because the IP of CH_3, 9.84 eV,[28] is much higher than

(21) Ervin, K.; Armentrout, P. B. *J. Chem. Phys.* **1985**, *83*, 166–189.
(22) Sunderlin, L.; Armentrout, P. B. *J. Phys. Chem.* **1988**, *92*, 1209–1219.
(23) Gioumousis, G.; Stevenson, D. P. *J. Chem. Phys.* **1958**, *29*, 294.
(24) Armentrout, P. B. In *Structure, Reactivity and Thermochemistry of Ions*; Ausloos, P., Lias, S. G., Eds.; D. Reidel: Dordrecht, The Netherlands, 1987; pp 97–164.
(25) Electronic state energies for Co^+ and Ni^+ are taken from: Sugar, J.; Corliss, C. *J. Phys. Chem. Ref. Data* **1985**, *14* (*Suppl. 2*). Those for Cu^+ are taken from: Chase et al. *J. Phys. Chem. Ref. Data* **1985**, *14* (*Suppl. 1*).
(26) Chesnavich, W. J.; Bowers, M. T. *J. Phys. Chem.* **1979**, *83*, 900–905.
(27) Weber, M. E.; Elkind, J. L.; Armentrout, P. B. *J. Chem. Phys.* **1986**, *84*, 1521–1529.

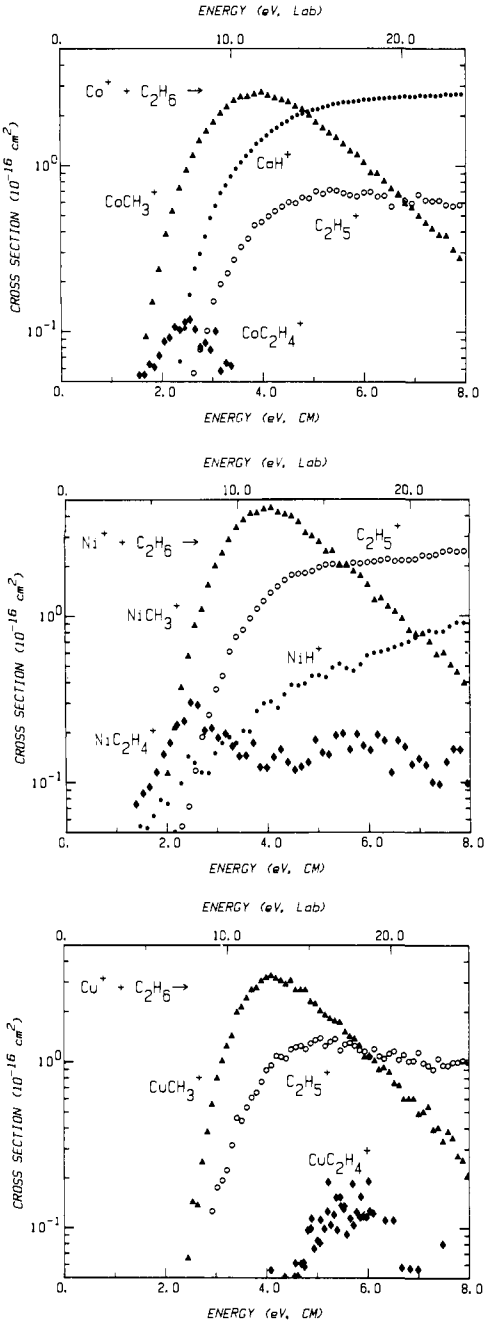

Figure 1. Variation of product cross section with translational energy in the laboratory frame (upper scale) and in the center of mass frame (lower scale) for the reaction of $Co^+ + C_2H_6$ (a), $Ni^+ + C_2H_6$ (b), and $Cu^+ + C_2H_6$ (c).

that of the MCH_3 product. These results are in reasonable agreement with the previously reported results of AB for Co^+ and HAB for Ni^+. The major exception concerns the $C_2H_5^+$ product, which AB did not report and HAB reported as a minor product. These discrepancies are presumably due to the difficulty in efficiently collecting the alkyl ion products.

The cross sections of MCH_3^+ where M = Co, Ni, and Cu are quite similar except for the differences in the reaction thermochemistry. The cross sections rise from threshold, peak, and then decline as is typical of endothermic reactions. The differences in the thresholds are determined exclusively by the variation in the metal ion–methyl bond strengths. The peak and falloff behavior of all three cross sections is almost identical. This is expected since the position of the peak is determined only by $D°(CH_3–CH_3) = 3.9$ eV. The similar shape of the cross sections suggests that the dynamics of these reactions is also similar. For reactions with larger alkanes, the behavior of the MCH_3^+ products follows a pattern similar to that shown here for ethane.

As the metal is changed, there is a distinct change in the relative amounts of the C–H bond cleavage channels (reactions 2 and 4). Since the only difference between these channels is the location of the charge, this change must be a direct result of the relative ionization potentials, namely, IP(CoH) < IP(C_2H_5) < IP(NiH) < IP(CuH). It is interesting to note that the sum of the cross sections for reactions 2 and 4 is similar for all three systems. Further, the relative probability of C–H bond cleavage (reactions 2 and 4) compared with C–C bond cleavage (reaction 1) does not change appreciably as the metal is changed.

The high-energy behavior of reactions 2 and 4 is distinct from that of reaction 1. Rather than peaking at the neutral bond dissociation energy, the MH^+ cross sections level off at higher energies. This is typical of metal–hydride ions formed in alkane reactions[15,29] and indicates that much of the excess energy in this reaction is carried off by the alkyl neutral product or is in translational energy. Likewise, the $C_2H_5^+$ cross section also levels out at high energies and shows no sign of dissociation, even though it can form $C_2H_3^+ + H_2$ beginning 2.2 eV above its threshold. This observation suggests that most of the excess energy is in translation.

Two minor product ions are observed in these reactions. First is MCH_2^+, observed at high energies for M = Co and Ni, where it is a minor decomposition channel of $MCH_3^+ \rightarrow MCH_2^+ + H$. There is also some evidence for the reaction, $M^+ + C_2H_6 \rightarrow MCH_2^+ + CH_4$, at lower energies for M = Co and Ni. Unambiguous identification of this reaction channel is hindered because of the difficulties in resolving this ion from the much larger MCH_3^+ product. We conclude that this process may be occurring but is a very insignificant reaction.

The second minor product channel is dehydrogenation of ethane, process 11, observed for all three metal ions (Figure 1). All three cross sections clearly behave as endothermic reactions, even though

$$M^+ + C_2H_6 \rightarrow MC_2H_4^+ + H_2 \qquad (11)$$

the reaction is exothermic for M = Co and Ni and probably Cu.[30] A comparable behavior has also been observed for this reaction where M = Fe.[15] This behavior cannot be due to formation of 2H (rather than H_2) since this reaction is endothermic by ≈2.5 eV for Co^+ and Ni^+. Rather there must be an activation barrier to reaction 11 somewhere along the potential energy surface for reaction. Because of the small size of the cross sections, the threshold for this reaction cannot be accurately determined. For Co and Ni, however, the apparent threshold is less than 1 eV and could be considerably less.

The cross sections for reaction 11 peak at 2.2, 2.5, and 5.5 eV for M = Co, Ni, and Cu, respectively. The position of these peaks is expected to correlate with the onset of competing reactions. For Co^+ and Ni^+, it can be noted that the peak occurs at the onset for formation of MH^+ or $C_2H_5^+$. This is consistent with the previously proposed reaction mechanism,[4] which suggests that MH^+, $C_2H_5^+$, and $MC_2H_4^+$ are all formed via the same intermediate, $H–M^+–C_2H_5$. For Cu^+, the peak occurs at much higher energies. Additional experiments with CH_3CD_3 confirm that this product signal is not due to impurities in the ethane or in the vacuum chamber. Further, these experiments show that while HD elimination dominates, losses of H_2 and D_2 are also observed with intensities of ~30% that for HD loss. This unusual behavior for $CuC_2H_4^+$ is discussed further below.

Propane. The experimental results for reaction of the three metal ions with propane are shown in Figure 2. The reactions of Co^+ and Ni^+ with propane yield analogous products, as pre-

(28) Schultz, J. C.; Houle, F. A.; Beauchamp, J. L. *J. Am. Chem. Soc.* **1984**, *106*, 3917–3927.

(29) Aristov, N. A.; Armentrout, P. B. *J. Am. Chem. Soc.* **1986**, *108*, 1806–1819.

(30) Hanratty et al.[19] give $D°(Co^+–C_2H_4) = 46 \pm 8$ kcal/mol and $D°(Ni^+–C_2H_4) = 48$ kcal/mol, while dehydrogenation of ethane requires only 32.5 kcal/mol. $D°(Cu^+–C_2H_4)$ is probably not very different from the values for Co and Ni.

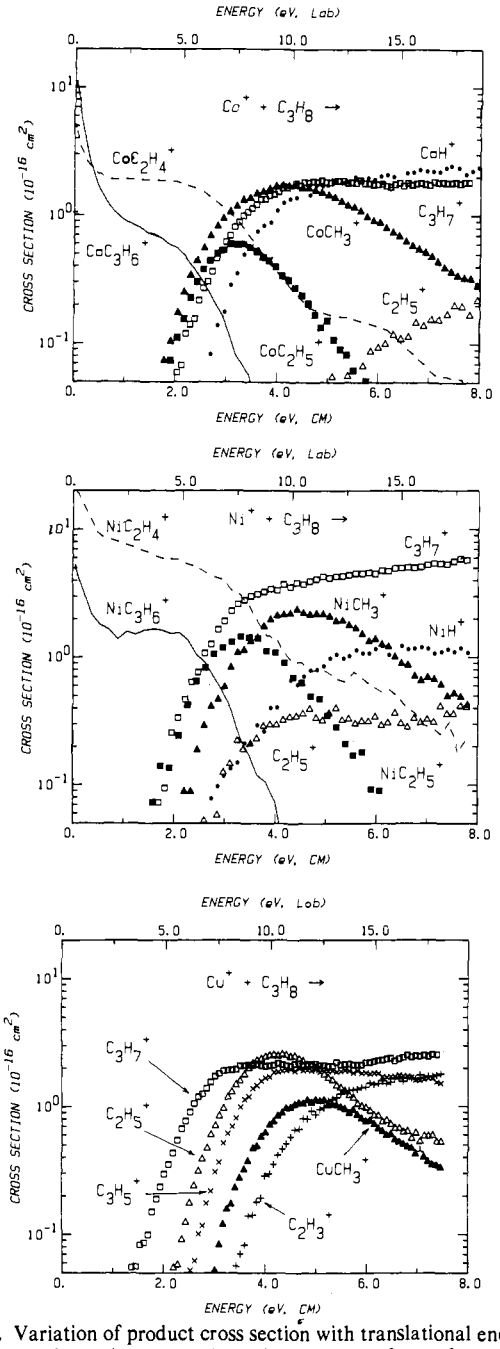

Figure 2. Variation of product cross section with translational energy in the laboratory frame (upper scale) and in the center of mass frame (lower scale) for the reaction of $Co^+ + C_3H_8$ (a), $Ni^+ + C_3H_8$ (b), and $Cu^+ + C_3H_8$ (c).

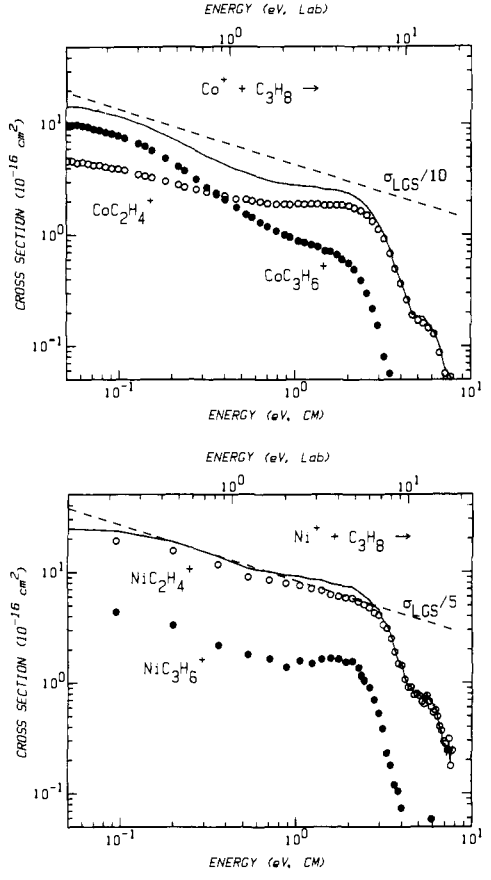

Figure 3. Cross sections for exothermic reactions of Co^+ (a) and Ni^+ (b) with propane to form $MC_2H_4^+$ (open circles) and $MC_3H_6^+$ (closed circles) as a function of kinetic energy in the laboratory frame (upper scale) and in the center of mass frame (lower scale). Solid lines show the sum of the two cross sections for each metal. Dashed lines show σ_{LGS} (eq 6) divided by 10 (a) and divided by 5 (b).

viously noted by HAB. The major endothermic product channels are reactions 1–4 for all three ions (although CuH^+ is not abundant). There are also a number of other endothermic reaction channels. For Co^+ and Ni^+ but not Cu^+, formation of $MC_2H_5^+$ is observed. For all three ions, formation of $C_2H_3^+$ and $C_3H_5^+$ is observed (though only plotted in Figure 2c) at higher energies. These products are presumed to be due to decomposition of the primary alkyl ion products, $C_2H_5^+$ and $C_3H_7^+$.

As in the ethane system, the relative amounts of metal–hydride and metal–alkyl ions, formed in reactions 1 and 2, compared to alkyl ion products, formed in reactions 3 and 4, provide qualitative information regarding the relative ionization potentials of the neutral species. It is clear from Figure 2 that IP(2-C_3H_7) < IP(CoH) < IP(NiH) < IP(CuH). Further, one can discern that IP($CoCH_3$) < IP($NiCH_3$) < IP(C_2H_5) < IP($CuCH_3$). Also, it is interesting to note that while the apparent thresholds for $CoCH_3^+$ and $CoC_2H_5^+$ are similar, $NiC_2H_5^+$ has a lower threshold than $NiCH_3^+$. This suggests that $CoC_2H_5^+$ is the metal–ethyl ion but that $NiC_2H_5^+$ may have a different structure, e.g., $H–Ni^+–C_2H_4$.

Both Co^+ and Ni^+ react exothermically with propane by eliminating stable molecules to produce metal–alkene ions, reactions 12 and 13. These cross sections are shown in somewhat

$$M^+ + C_3H_8 \rightarrow MC_3H_6^+ + H_2 \quad (12)$$

$$\rightarrow MC_2H_4^+ + CH_4 \quad (13)$$

more detail in Figure 3. Cu^+ is clearly distinct in that it undergoes neither of these exothermic reactions. This is in agreement with the failure to observe any reaction of Cu^+ with propane in ICR experiments.[31]

One very interesting point, which has not been commented on previously, is that the energy dependence of these exothermic cross sections is quite different for Co^+ and Ni^+. For the case of Co^+, our results show that reaction 12 is favored below ~0.3 eV. We measure a branching ratio of $CoC_2H_4^+$ to $CoC_3H_6^+$ of 33/67 at the lowest energies (<0.1 eV). This is consistent with previous work where AB report a branching ratio of 25/75 at ~0.5 eV,[4] and at thermal energies, Jacobson and Freiser measure 31/69 by *FTMS*,[20b] and Tonkyn et al. measure 24/76 in a flow tube.[32] At higher energies, the branching ratio favors $CoC_2H_4^+$, by 75/25 at ≈1 eV. This is in qualitative agreement with the results of AB. Note that the reaction proceeds at only ≃8% of the predicted LGS collision rate, eq 6, at the lowest energies.

For Ni^+ with propane, $NiC_2H_4^+$ is favored at all energies (Figure 3b). Below ~1 eV, the energy dependence of both cross sections agrees well with the $E^{-0.5}$ prediction of eq 6, and the rate

(31) Kappes, M. M. Ph.D. Thesis, MIT, 1981.
(32) Tonkyn, R.; Ronan, M.; Weisshaar, J. C. *J. Phys. Chem.* **1988**, *92*, 92–102.

is ~20% of the LGS magnitude. We measure a branching ratio of $NiC_2H_4^+$ to $NiC_3H_6^+$ of 78/22 for reaction energies below 1 eV. This agrees well with the branching ratios reported by HAB, 80/20 at ~1 eV,[17] Jacobson and Freiser, 80/20 at thermal energies,[20b] and Tonkyn et al., 83/17 at thermal energies.[32]

It is also interesting to note that at higher energies, there is a new feature appearing in the cross sections for $CoC_2H_4^+$ and $NiC_2H_4^+$. This begins between 4 and 5 eV in both the Co^+ system and the Ni^+ system (Figures 2 and 3). We attribute this feature to reaction 14, a decomposition channel of the $MC_2H_5^+$ product.

$$M^+ + C_3H_8 \rightarrow MC_2H_5^+ + CH_3 \rightarrow MC_2H_4^+ + H + CH_3 \quad (14)$$

Note that this process cannot begin until ≈3.3 eV, 4.54 eV = $D°(H-CH_3)$ higher in energy than reaction 13.

Isobutane. The experimental cross sections for the most prominent reaction products in the reactions of the metal ions with isobutane are shown in Figure 4. For Co^+ and Ni^+, the main products observed are the same as reported by AB and HAB, although some differences in relative magnitudes are observed. In particular, we find that the cross sections for reactions 1–4 have comparable magnitudes, while in previous work the alkyl ion cross sections were significantly smaller. We also observe minor decomposition products, such as $C_2H_5^+$ and $C_2H_3^+$, at higher energies which have not been reported previously. Cu^+ reacts with isobutane (Figure 4c) to form many of the same endothermic alkyl ion products, but metal-containing product ions are much less abundant. The formation of $NiC_2H_4^+$ and $CuC_2H_4^+$ are both unusual products which appear to involve rather extensive reorganizations of the alkane.

Comparison of the apparent thresholds of the alkyl vs metal-containing ions continues the ionization potential trend established with smaller alkanes. It is clear that IP(2-C_3H_7) is slightly lower than IP($CoCH_3$) and significantly lower than IP($NiCH_3$) and IP($CuCH_3$). Similarly, IP(t-C_4H_9) is significantly less than that for any of the metal–hydrides. Note that the apparent threshold for CoH^+ is definitely higher than that for $C_4H_9^+$, but the magnitude of the CoH^+ product exceeds that for $C_4H_9^+$ above 4.5 eV. This is presumably because Co^+ can extract a hydrogen atom from either the tertiary or the primary carbons of isobutane with equal facility since the bond energies differ by only 0.22 eV. However, H^- abstraction from the tertiary position is favored by 1.45 eV over that from the primary position. Thus, CoH^+ can be formed by using any of the 10 hydrogen atoms, while $C_4H_9^+$ formation is essentially restricted to the single tertiary hydrogen.

Exothermic demethanation, reaction 16, is preferred over dehydrogenation, reaction 15, for both Ni^+ and Co^+ at all energies. The cross sections have similar energy dependence, falling off as

$$M^+ + CH(CH_3)_3 \rightarrow MC_4H_8^+ + H_2 \quad (15)$$

$$\rightarrow MC_3H_6^+ + CH_4 \quad (16)$$

approximately $E^{-0.5}$ at the lowest energies, <0.5 eV. We measure branching ratios for $MC_3H_6^+$ to $MC_4H_8^+$ of 92/8 for Ni^+. These compare well with the results of previous work by HAB, 89/11,[17] and by Freas and Ridge, 88/12.[33] For Co^+, we find a ratio of 83/17, in good agreement with the results of AB, 77/23,[4] and Freas and Ridge, 85/15.[33] Again, Cu^+ does not effect either of these exothermic reactions; however, the adduct $Cu(C_4H_{10})^+$ is observed in yields that are only somewhat smaller than the exothermic cross sections for reaction of Co^+. In these experiments, the presence of the neutral reactant is sufficiently low that it is unlikely that the adduct is formed via secondary collisional stabilization. Thus, we believe that this species is formed in a single bimolecular event but has a lifetime longer than the flight time of the ions to the mass filter, tens of microseconds.

Neopentane. In reaction of Co^+ and Ni^+ with neopentane, Figure 5a and 5b, the most prominent features are exothermic demethanation, reaction 17. The largest endothermic processes

$$M^+ + C(CH_3)_4 \rightarrow MC_4H_8^+ + CH_4 \quad (17)$$

(33) Freas, R. B.; Ridge, D. P. *J. Am. Chem. Soc.* **1980**, *102*, 7129–7131.

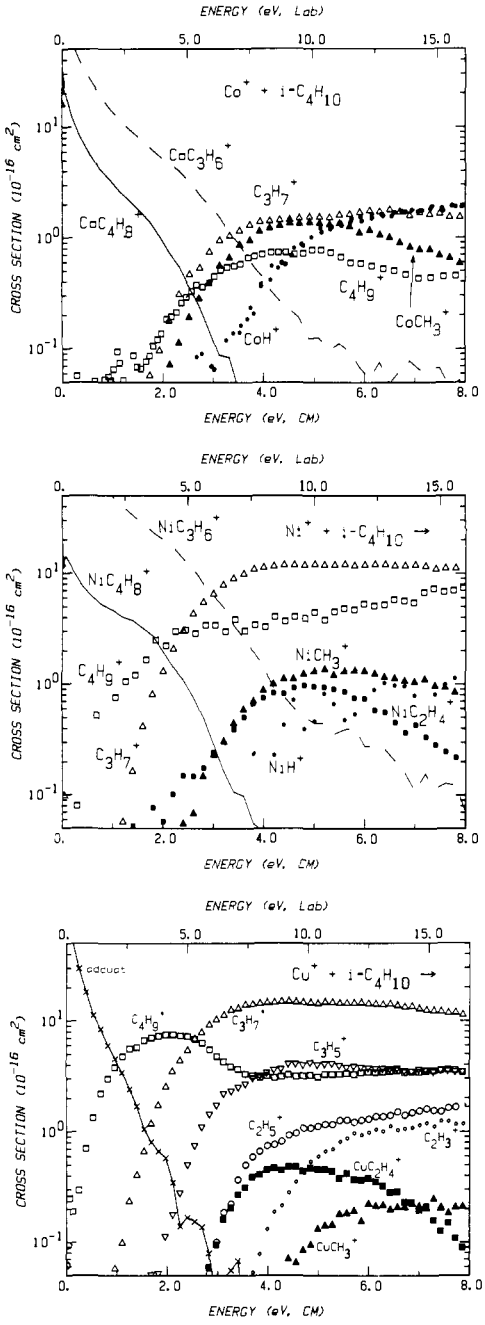

Figure 4. Variation of product cross section with translational energy in the laboratory frame (upper scale) and in the center of mass frame (lower scale) for the reaction of $Co^+ + i$-C_4H_{10} (a), $Ni^+ + i$-C_4H_{10} (b), and $Cu^+ + i$-C_4H_{10} (c).

are reaction 3, clearly indicating that IP(t-C_4H_9) < IP($CoCH_3$) and IP($NiCH_3$). Reactions 1 and 2 occur in lower yields. We also observe a number of other endothermic products ($C_2H_5^+$, $C_3H_5^+$, and $C_3H_7^+$), which presumably result from decomposition of $C_4H_9^+$. Our results for these processes are in reasonable agreement with the results of AB and the observation by HAB that reaction 17 is the only exothermic process for Ni^+.

The reaction of Cu^+ with neopentane yields a collection of products similar to that for Co^+ (Figure 5c). The alkyl ion products ($C_2H_5^+$, $C_3H_5^+$, $C_3H_7^+$, and $C_4H_9^+$) are about an order of magnitude larger than in the Co^+ system, while the cross section for $CuCH_3^+$ is extremely small (off scale in Figure 5c) and shifted to high energy. We observe formation of $C_5H_{11}^+$ (reaction 2) with an apparent threshold of ~2 eV, a reaction that has not been reported for any metal ion reaction with neopentane.

Interestingly, reaction 17 is observed for Cu^+ although the reaction appears to be slightly endothermic, as does reaction 3,

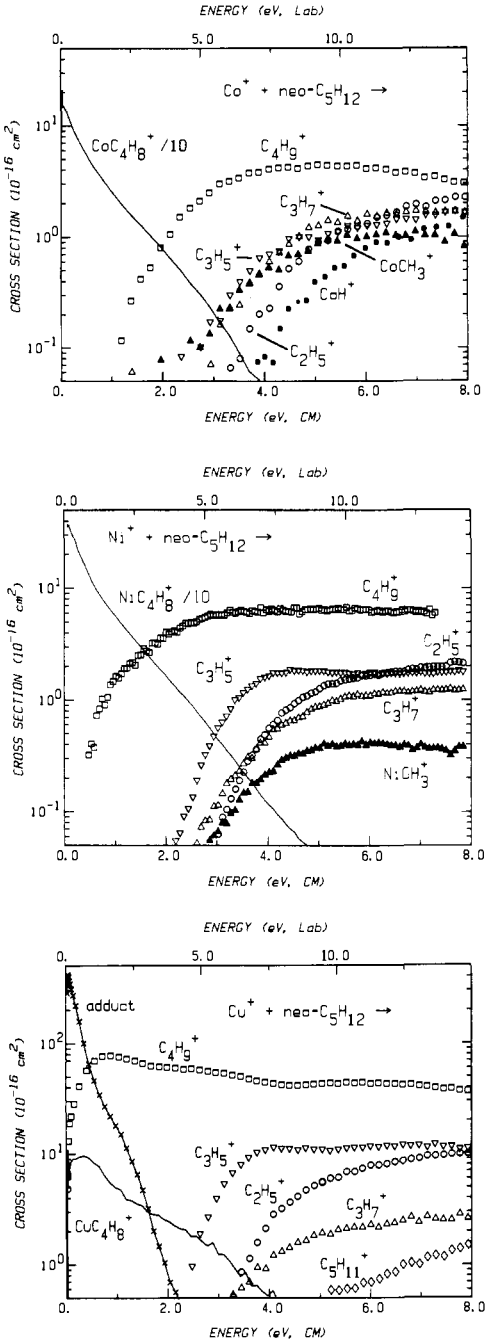

Figure 5. Variation of product cross section with translational energy in the laboratory frame (upper scale) and in the center of mass frame (lower scale) for the reaction of Co^+ + neo-C_5H_{12} (a), Ni^+ + neo-C_5H_{12} (b), and Cu^+ + neo-C_5H_{12} (c).

formation of $C_4H_9^+$. The only exothermic reaction is formation of the adduct $Cu(C_5H_{12})^+$. These reactions are in competition with one another since the cross section for the adduct rapidly decreases as soon as reaction 3 becomes energetically available. This is further demonstrated by noting that the total cross section closely follows the LGS prediction, eq 6, from our lowest energies to ~2 eV. This is evidence that the adduct is not formed via collisional stabilization but that its lifetime exceeds the flight time to the mass filter.

Thermochemistry

Derivation of Thermochemical Values. The cross sections for reactions 1–4 are subjected to detailed threshold analysis as described in the experimental section. The results are summarized in Tables I–III. Accurate determination of MH^+ thresholds in these systems is hindered by experimental difficulties in resolving the small product intensity from the $\simeq 10^5$ times larger reactant ion beam intensity. Further, in the Ni and Cu systems, reaction 2 generally has a very small cross section. Thus, threshold analyses of the metal–hydride cross sections were performed only for Co.

Bond dissociation energies for the metal-containing product species can be calculated from eq 18–21, where $E_0(x)$ is the

Table I. Parameters in eq 7 Used for Fitting Co^+ Reaction Cross Sections

ionic product	n	E_T, eV	σ_0	E_D, eV	p
		Ethane			
$CoCH_3^+$	1.75 ± 0.15	1.70 ± 0.15	3.00 ± 0.15	3.9	3
CoH^+	1.2 ± 0.10	2.48 ± 0.05	2.73 ± 0.20		
$C_2H_5^+$	1.2 ± 0.1	2.60 ± 0.06	1.15 ± 0.12	4.8	
		Propane			
$CoCH_3^+$	1.66 ± 0.07	1.73 ± 0.06	2.10 ± 0.20	4.1	2
CoH^+	1.0	3.05 ± 0.27	3.01 ± 0.20		
$C_2H_5^+$	2.37 ± 0.5	<2.97 ± 0.33	0.04 ± 0.01	7.7	1
$C_3H_7^+$	2.22 ± 0.10	1.80 ± 0.10	1.10 ± 0.40	3.8	1
		Isobutane			
$CoCH_3^+$	1.59 ± 0.11	2.13 ± 0.08	1.68 ± 0.09	4.8	2
CoH^+	1.0	3.50 ± 0.30	3.48 ± 0.50		
$C_3H_7^+$	2.94 ± 0.14	1.19 ± 0.10	0.39 ± 0.05	3.4	1
$C_4H_9^+$	2.8 ± 0.30	0.77 ± 0.19	0.14 ± 0.05	3.9	2
		Neopentane			
$CoCH_3^+$	2.0	2.00 ± 0.30	0.40 ± 0.10		
CoH^+	1.0	3.00 ± 0.30	2.70 ± 0.50		
$C_4H_9^+$	2.75 ± 0.27	0.65 ± 0.17	0.17 ± 0.32		

Table II. Parameters in eq 7 Used for Fitting Ni^+ Reaction Cross Sections

ionic product	n	E_T, eV	σ_0	E_D, eV	p
		Ethane			
$NiCH_3^+$	2.4 ± 0.2	1.90 ± 0.10	4.2 ± 0.8	3.8	3
$C_2H_5^+$	1.8 ± 0.2	2.32 ± 0.15	2.0 ± 0.8	5.1	1
		Propane			
$NiCH_3^+$	2.5 ± 0.3	1.96 ± 0.15	1.1 ± 0.2	4.2	3
$C_2H_5^+$	2.0 ± 0.2	2.13 ± 0.15	0.4 ± 0.2	4.0	1
$C_3H_7^+$	2.4 ± 0.2	1.45 ± 0.16	1.8 ± 0.4	3.7	0
		Isobutane			
$NiCH_3^+$	2.1 ± 0.5	2.10 ± 0.20	0.8 ± 0.2	5.1	2
$C_3H_7^+$	2.8 ± 0.4	1.10 ± 0.15	3.3 ± 1.2	3.2	1
$C_4H_9^+$	2.0 ± 0.2	0.55 ± 0.20	2.0 ± 0.4	2.0	0
		Neopentane			
$NiCH_3^+$	1.7 ± 0.5	2.24 ± 0.20	0.3 ± 0.1		
$C_4H_9^+$	1.7 ± 0.2	0.38 ± 0.12	3.2 ± 0.6		

Table III. Parameters Used in eq 7 for Fitting Cu^+ Reaction Cross Sections

ionic product	n	E_T, eV	σ_0	E_D, eV	p
		Ethane			
$CuCH_3^+$	1.6 ± 0.1	2.60 ± 0.07	6.9 ± 1.1	3.9	2
$C_2H_5^+$	2.5 ± 0.2	2.23 ± 0.20	1.0 ± 0.5	4.0	1
		Propane			
$CuCH_3^+$	2.2 ± 0.2	2.78 ± 0.15	1.5 ± 0.2	4.7	3
$C_2H_5^+$	2.6 ± 0.2	2.10 ± 0.20	2.2 ± 0.9	4.0	
$C_3H_7^+$	2.8 ± 0.2	1.36 ± 0.20	1.2 ± 0.5		
		Isobutane			
$CuCH_3^+$	2.1 ± 0.5	2.10 ± 0.20	0.8 ± 0.2	5.8	1
$C_3H_7^+$	3.0 ± 0.4	0.92 ± 0.16	6.5 ± 2.5	3.0	1
$C_4H_9^+$	1.7 ± 0.2	0.27 ± 0.20	6.9 ± 2.6	1.5	0
		Neopentane			
$C_4H_9^+$	0.6 ± 0.1	0.20 ± 0.05	75 ± 10		
$C_5H_{11}^+$		~2			

$$D°(M^+-CH_3) = D°(R-CH_3) - E_0(1) \quad (18)$$

$$D°(M^+-H) = D°(R-H) - E_0(2) \quad (19)$$

$$D°(M-CH_3) = D°(R-CH_3) + IP(R) - IP(M) - E_0(3) \quad (20)$$

$$D°(M-H) = D°(R-H) + IP(R) - IP(M) - E_0(4) \quad (21)$$

reaction endothermicity for reaction x. These equations assume no activation barriers in excess of the reaction endothermicity, which is a reasonable assumption for most ion–molecule reactions.[24,34] Thermochemistry for the alkane species as well as the ionization potentials of the metals and the various radicals are generally known (Table IV). However, the heats of formation of hydrocarbon radicals are still a source of controversy. We have chosen to use the values taken from recent studies of Gutman and co-workers[35] and several references cited therein.[36] These values provide a consistent set of R–H and R–CH_3 bond energies and, when combined with the ionization potentials given in Table IV, are consistent with established ion thermochemistry.[37]

Thermochemical data derived from the results of the various alkane reactions are summarized in Table V. Our ability to obtain reliable thermochemistry from eq 18–21 can be hindered by two problems. One problem, discussed in the Experimental Section, is the ability to accurately determine the threshold by effectively modeling the cross section. The second problem concerns whether the reaction thresholds observed correspond to the thermodynamic limit. Deviations from thermodynamic behavior may occur if there is a barrier in excess of the endothermicity for the reaction. Alternatively, the thermodynamic thresholds may be obscured if there are processes that strongly compete with the endothermic reaction of interest. The resulting cross-section thresholds may be very strongly perturbed, challenging our modeling abilities.

By inspection of reactions 1–4, we can expect strong competition between reactions 1 and 3 and between 2 and 4. We see from eq 18 and 19 and the data in Table IV that the endothermicity of reactions 1 and 2 should vary only slightly as R is increased. This is because the C–C and C–H bond dissociation energies differ by only a few kilocalories per mole for the alkanes of this study. The experimental results for reaction 1 (M = Co) for R increasing from methyl to *tert*-butyl radical are shown in Figure 6. For small R, the cross sections increase rapidly from threshold; but as R gets larger, the cross sections begin to rise more slowly such that the threshold is much more difficult to accurately identify. There is also an accompanying shift in the peak position, E_D, to higher energies. This is presumably because as more degrees of freedom are available in the R products, excess energy goes into these internal modes rather than into those of MCH_3^+. Only the latter lead to product dissociation. A decrease in the cross-section magnitudes is also observed. These effects are also observed for Ni^+ and Cu^+ reactions and are reflected in the fitting parameters, E_T, σ_0, and E_D, given in Tables I–III.

On the basis of eq 20 and 21, formation of R^+ or RCH_2^+ in reactions 3 and 4 are expected to become markedly more favorable as the alkyl size increases. This is because the ionization potential of R decreases substantially as the alkane size increases (Table IV). The threshold for reaction 3 with isobutane, for example, is expected to shift down in energy by 1.53 eV relative to the threshold for reaction 3 with ethane. The cross sections for reactions 3 and 4 show behavior opposite to that seen for reactions 1 and 2; i.e., the threshold energies and peak positions shift to lower energies and the cross sections generally increase in magnitude as R increases in size. These effects are observed for all three ions and are reflected in the fitting parameters, E_T, σ_0, and E_D, given in Tables I–III.

Thus, the experimental results indicate that reactions 1 and 2 become less favored as R increases while formation of the alkyl products, reactions 3 and 4, become more favored. This supports the idea that there is strong competition between reactions 1 and 3 and between reactions 2 and 4, which must be kept in mind when

Table IV. Literature Thermochemical Data (kcal/mol) at 298 K

R	$\Delta_f H°(R)$[a]	$D°(R-H)$[b]	$D°(R-CH_3)$[b]	IP(R),[c] eV
CH_3	34.8 (0.2)	104.8 (0.2)	89.6 (0.3)	9.84 (0.02)
C_2H_5	28.3 (0.7)	100.4 (0.7)	88.1 (0.7)	8.13 (0.06)
2-C_3H_7	21.0 (0.7)	98.1 (0.7)	87.9 (0.7)	7.36 (0.02)
t-C_4H_9	11.5 (0.7)	95.7 (0.7)	86.5 (0.7)	6.70 (0.03)
1-C_3H_7	22.6 (1.1)[d]	99.7 (1.1)		8.09 (0.01)
i-C_4H_9	16[e]	100.2		7.93
Co				7.86 (0.06)
Ni				7.638 (0.001)
Cu				7.726 (0.001)

[a] Except where noted, radical heats of formation are taken from ref 35 and 36. See text for a discussion of these values. [b] Bond energies are derived from $\Delta_f H°(H)$ = 52.1 kcal/mol, the alkyl heats of formation given here, and alkane heats of formation given by: Pedley, J. M.; Naylor, R. D.; Kirby, S. P. *Thermochemical Data of Organic Compounds*; Chapman and Hall: London, 1986. [c] Ionization potentials in eV. Values for radicals are taken from ref 37. Values for the metals are taken from ref 25. [d] Marshall, R. M.; Rahman, L. *Int. J. Chem. Kinet.* **1977**, *9*, 705. [e] Reference 37.

Table V. Thermochemistry Obtained in This Study (kcal/mol)[a]

	$D°(Co^+-CH_3)$	$D°(Co-CH_3)$	$D°(Co-H)$	$D°(Co^+-H)$
ethane	49.1 (3.5)		45.5 (2.4)	[42 (2)]
propane	46.9 (1.9)	[>24 (8)]	43.8 (3.0)	[27 (2)]
isobutane	[38 (2)]	47.7 (3.0)	50.1 (4.8)	[14 (7)]
neopentane	[39 (7)]	43.7 (4.4)		---
	$D°(Ni^+-CH_3)$	$D°(Ni-CH_3)$		$D°(Ni-H)$
ethane	45.0 (2.4)			57.3 (3.7)
propane	41.8 (3.7)	[50 (4)]		57.4 (3.7)
isobutane	[39 (5)]	55.3 (3.7)		60.6 (4.8)
neopentane	[34 (5)]	55.3 (3.1)		
	$D°(Cu^+-CH_3)$	$D°(Cu-CH_3)$		$D°(Cu-H)$
ethane	29.7 (1.7)			58.2 (5.0)
propane	[24 (4)]	[49 (5)]		58.3 (4.8)
isobutane	[8 (4)]	58.3 (3.9)		65.9 (4.8)
neopentane	---	58.2 (1.8)		---

[a] Bond energies for individual alkane systems are calculated by using eq 18–21. Dashed lines indicate no value is available. Blanks indicate the reaction was not observed. Square brackets indicate the value is not used in the average values listed in Table VI.

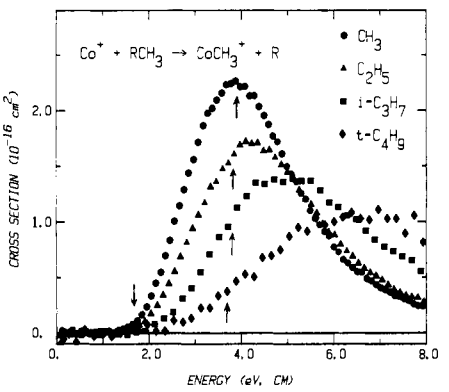

Figure 6. Variation in the experimental cross section for reaction 1, where R = CH_3 (circles), C_2H_5 (triangles), 2-C_3H_7 (squares), and t-C_4H_9 (diamonds). The arrow pointing down indicates the measured threshold for the reaction with ethane (R = CH_3). Upward arrows indicate the C–C bond dissociation energies for ethane (3.89 eV), propane (3.82 eV), isobutane (3.79 eV), and neopentane (3.69 eV).

(34) Talrose, V. L.; Vinogradov, P. S.; Larin, I. K. In *Gas Phase Ion Chemistry*; Bowers, M. T., Ed.; Academic: New York, 1979; Vol. 2, pp 305–347.

(35) Russell, J. J.; Seetula, J. A.; Timonen, R. S.; Gutman, D.; Nava, D. F. *J. Am. Chem. Soc.* **1988**, *110*, 3084–3091. Russell, J. J.; Seetula, J. A.; Gutman, D. *J. Am. Chem. Soc.* **1988**, *110*, 3092–3099.

(36) Canosa, C. E.; Marshall, R. M.; Sheppard, A. *Int. J. Chem. Kinet.* **1981**, *13*, 295. Pacey, P. D.; Wimalasena, J. H. *J. Phys. Chem.* **1984**, *88*, 5657–5660. Cao, J.-R.; Back, M. H. *Int. J. Chem. Kinet.* **1984**, *16*, 961. Brouard, M.; Lightfoot, P. D.; Pilling, M. J. *Ibid.* **1986**, *90*, 445–450.

(37) Lias, S. G.; Bartmess, J. E.; Liebman, J. F.; Holmes, J. L.; Levin, R. D.; Mallard, W. G. *J. Phys. Chem. Ref. Data* **1988**, *17* (*Suppl. 1*).

Table VI. Summary of M–H and M–CH_3 Bond Energies (kcal/mol) at 298 K[a]

M	$D°(M^+–H)$	$D°(M^+–CH_3)$	$D°(M–H)$	$D°(M–CH_3)$
Co	46.6 (1.4)[b]	49.1 (3.5)	46 (3)	46 (3)
	51 (5)[c]	61 (4)[c]	39 (6)[c]	41 (10)[c]
	45.4[d]	49.8[d]	45.0[d]	39.9[d]
		>56, <68[e]	45 (3)[f]	
		57 (7)[g]	42 (3)[h]	
		46 (14)[i]	54 (10)[j]	
			[74][k]	
Ni	39.5 (1.8)[b]	45.0 (2.4)	58 (3)	55 (3)
	41.9[d]	41.3[d]	62.1[d]	53.7[d]
	43 (2)[l]	48 (5)[l]	59 (2)[f]	60[m]
		<56[e]	65 (6)[j]	
			<71[k]	
Cu	22.1 (3.0)[b]	29.7 (1.7)	61 (4)	58 (2)
	19.4[d]	30.3[d]	60.9[d]	50.5[d]
			60 (1)[f]	>59 [>48][n]
			63 (1)[k]	
Fe	49.8 (1.4)[o]	57.9 (2.4)[p]	46 (3)[p]	37 (7)[q]
	53.2[d]	54.6[d]	38.7[d]	34.9[d]
			>30 (3)[h]	
Zn	55 (3)[r]	71 (3)[s]	20 (1)[k]	19 (3)[s]

[a] Unless specified otherwise, the values are from this work and are the average of the values listed in Table V excluding those values in square brackets. See text for discussion. Uncertainties are given in parentheses. [b] Reference 16. [c] Reference 4. [d] Reference 38. [e] Reference 7. [f] Reference 11. [g] Reference 8. [h] Reference 13. [i] Reference 40. [j] Reference 12. [k] Reference 10. [l] Reference 17. [m] Reference 41. [n] Reference 42. The value in brackets is calculated from the results of ref 42 but uses more recent thermochemistry as discussed in the text. [o] Elkind, J. L.; Armentrout, P. B. *J. Phys. Chem.* **1986**, *90*, 5736–5745. [p] Reference 15. [q] Schultz, R. H.; Armentrout, P. B., work in progress. [r] Reference 48. [s] Reference 14a.

considering the results in Table V. Since reactions 1 and 2 are strongly disfavored for the larger alkane systems, we expect *decreasingly* reliable thermodynamic information for MCH_3^+ and MH^+ as R increases in size. Thus, threshold energies from the larger alkanes can be viewed as upper limits to the thermodynamic onset and the ionic bond energies subsequently lower limits. Our best determination for the metal–methyl ionic bond energies is therefore derived from the ethane reaction alone.

By the same token, we expect the most reliable neutral thermochemistry from the larger alkane reactions where the competition favors the endothermic process of interest. However, the efficient collection of alkyl ions is generally difficult, especially as threshold energies shift to lower values for the larger alkanes. This contributes to difficulties in the interpretation of the cross sections. As the number of degrees of freedom in the reactants increase, the accuracy of the thermochemistry obtained from threshold analyses may decrease. Therefore, large alkane systems are not used as exclusive sources of neutral thermochemistry. Within experimental error, the results of the threshold analyses are generally self-consistent for all the alkanes studied (Table V). These are averaged together to obtain the best determination of the neutral bond energies. The error limits on the final weighted average are conservative and estimated to reflect deviations observed in different alkane systems as well as other experimental errors.

Comparison with Previous Experimental Work: Ions. Table VI summarizes the thermochemical results of this work and also determinations of MH^+ bond energies from previous studies of reaction 5. In some cases, these numbers differ slightly from preliminary values published in a recent compilation.[2] Where available, results from previous experimental and theoretical studies are given for comparison. The thermochemistry derived here is in agreement with the more reliable measurements and with the recent calculations of Bauschlicher et al.[38] In some cases, discussed in detail below, our values substantially revise previous experimental determinations.

Of the ionic methyl species, $CoCH_3^+$ has seen the most study, followed by $NiCH_3^+$. No previous work on the thermochemistry of $CuCH_3^+$ exists. In 1975, Allison and Ridge[7] used ICR to study the reactions of methyl–halides with Co^+ produced by electron impact (EI) ionization of $Co(CO)_3NO$ and with Ni^+ produced by EI of $Ni(CO)_4$. They found that $CoCH_3^+$ was formed in the reaction with CH_3I but not CH_3Br, while $NiCH_3^+$ was not formed with either reactant. They therefore concluded that $D°(I–CH_3)$ = 56 kcal/mol < $D°(Co^+–CH_3)$ < 68 kcal/mol = $D°(Br–CH_3)$ and that $D°(Ni^+–CH_3)$ < 56 kcal/mol. Our value for $D°(Ni^+–CH_3)$ is consistent with these results, while the lower limit for $D°(Co^+–CH_3)$ is clearly inconsistent with the value of 49.1 ± 3.5 kcal/mol derived here. The accuracy of thermochemical bracketing depends on the assumption that ground-state metal ions account for the reactivity observed. In support of this assumption, Allison and Ridge noted that the measured reaction rates do not depend on the energy of the ionizing electrons. However, work in our laboratory using EI ionization of $Co_2(CO)_8$ (50-eV electron energy) finds evidence of excited states.[16] Therefore, we conclude that it is possible that excited states of Co^+ contribute to the reactivity in the ICR experiments. If the reactivity is due to the first excited state of Co^+ (at 0.48 eV),[25] then the lower bound for $D°(Co^+–CH_3)$ shifts to 45 kcal/mol. This interpretation is supported by a reexamination of the reactions of Co^+ with methyl halides.[39] These studies yield a value for $D°(Co^+–CH_3)$ of 48.8 ± 3.1 kcal/mol, in excellent agreement with the results reported here.

In 1981, AB reported $D°(CoCH_3^+)$ equal to 61 ± 4 kcal/mol, from an ion beam study of reaction 1 where R = CH_3. Note that this agrees with the limits determined by Ridge and Allison and hence disagrees with the present results. As noted above, our data and that of AB are in good agreement; however, our interpretation utilizes quite different parameters in eq 7. Thus, the difference between AB's value and that derived here is due to different interpretations of the reaction thresholds, which are quite sensitive to the precision of the data. The early data were not sufficiently precise to unambiguously determine the threshold without constraining the number of freely varying parameters in eq 7. With the improved ion beam technology currently available, this constraint has been largely removed. Note that there is much better agreement between our results for $D°(NiCH_3^+)$, 45.0 ± 2.4 kcal/mol, and that reported by HAB, 48 ± 5 kcal/mol, where the fitting parameters of eq 7 are more similar.

The other two literature values for $D°(CoCH_3^+)$ agree with the present value within their rather large uncertainties. Freiser and co-workers[8] reported a value for $D°(Co^+–CH_3)$ of 57 ± 7 kcal/mol from photodissociation studies of $CoCH_3^+$. The large uncertainty in this value is due to the difficulty in assigning the photodissociation threshold since the onset formation of Co^+ is not sharp. In another study, "the FTMS analogy of the ion beam experiment", Freiser and co-workers[40] reported 46 ± 14 kcal/mol from a study of reaction 1, Co^+ with ethane. In this study, there are inherent difficulties in determining the relative kinetic energy of interaction. Further errors may be introduced in the interpretation of the threshold by the assumption made that the ion intensity should rise linearly from threshold with kinetic energy.

Comparison with Previous Experimental Work: Neutrals. Fewer studies are available for the neutral thermochemistry. AB reported $D°(CoCH_3)$ = 41 ± 10 kcal/mol and $D°(CoH)$ = 39 ± 6 kcal/mol. These values are calculated from $IP(CoCH_3)$ and IP(CoH) values, which are estimated from relative product cross-section magnitudes of reactions 1 vs 3 and reactions 2 vs 4. AB's estimates agree with our values within their rather large experimental errors. In the case of $D°(CoH)$, AB found that in the reaction with propane, process 2 had a larger cross section than process 4, which was taken to indicate that IP(CoH) < $IP(2\text{-}C_3H_7)$ = 7.36 eV. Due to better collection of the alkyl ion

(38) Bauschlicher, C. W.; Langhoff, S. R.; Partridge, H.; Barnes, L. A. *J. Chem. Phys.* In press.

(39) Fisher, E. R.; Sunderlin, L. S.; Armentrout, P. B. *J. Phys. Chem.*, submitted for publication.

(40) Forbes, R. A.; Lech, L. M.; Freiser, B. S. *Int. J. Mass Spectrom. Ion Processes* **1987**, *77*, 107–121.

Table VII. Ionization Potentials (in eV) of MH and MCH_3[a]

	IP(M)	IP(MH)	IP(MCH_3)
Fe	7.90	7.7 (0.2)	7.0 (0.3)
Co	7.86	7.8 (0.2)	7.7 (0.2)
Ni	7.64	8.4 (0.2)	8.1 (0.2)
Cu	7.73	9.4 (0.2)	9.0 (0.2)
Zn	9.39	7.9 (0.2)	7.1 (0.2)

[a] Values for M are taken from Table IV. Values for MH and MCH_3 are calculated from the data in Table VI by using eq 23. Uncertainties are in parentheses.

product in the present study, we conclude the opposite. As can be seen in Figure 2a, we find that the magnitudes of these processes are comparable and that the formation of $C_3H_7^+$ clearly begins at a lower energy than CoH^+. Thus, AB's value is only a lower limit to the true bond energy.

Our results for all three neutral metal–hydrides are in excellent agreement with the values reported by Kant and Moon.[11] In the one case where the spectroscopic value is considered reliable, CuH, we also obtain good agreement. For CoH and NiH, our values are within experimental error of those determined by Tolbert and Beauchamp[12] and Sallans et al.[13] who used ion–molecule chemistry to bracket the values. The values are also in reasonably good agreement with the calculations of Bauschlicher et al.[38] Our values for the neutral metal–methyl bond energies are in poorer agreement with these calculated values, except in the case of $NiCH_3$, where our result of 55 ± 3 kcal/mol is in between the results of two ab initio calculations, 53.7[38] and 60 kcal/mol.[41] For $CoCH_3$ and $CuCH_3$, our values are somewhat higher than the calculated values,[38] which seems odd considering the good agreement for all the other Co and Cu bond energies.

Our value for $D°(CuCH_3)$ is somewhat lower than the lower limit of 59 kcal/mol cited by Weil and Wilkins.[42] These authors used FTMS to observe reaction 22, and assumed that only

$$Cu^+ + t\text{-}C_4H_9OH \rightarrow CuCH_3 + C_3H_6OH^+ \qquad (22)$$

ground-state exothermic reactions were involved. The discrepancy with our work is eliminated, however, when more recent thermochemical values for $\Delta_f H°(C_3H_6OH^+)$ are used.[37] These show that if reaction 22 is exothermic, then $D°(Cu\text{–}CH_3) > 48$ kcal/mol.

Ionization Potentials. Another way of checking the consistency of these results is via the relative ionization potentials (IPs) of these species. Based on the relative thresholds discussed in Results, we can conclude that the IPs have the following relative values: $t\text{-}C_4H_9 < 2\text{-}C_3H_7 < CoCH_3$, $CoH < NiCH_3 < C_2H_5 < NiH < CuCH_3 < CuH$. Table VII gives the IPs for the MH and MCH_3 species, which can be derived from the bond energies in Table VI by using eq 23 where X = H or CH_3. A comparison of these

$$IP(MX) = IP(M) + D°(M\text{–}X) - D°(M^+\text{–}X) \qquad (23)$$

values shows that they follow the relative values given above, as expected.

Periodic Trends. Of fundamental importance to the bonding of transition-metal species are the electronic state (orbital occupancy and spin state) and charge of the transition-metal atom and the nature of the ligand. As more complete and reliable thermochemistry for a range of metals and ligands becomes available these effects can be systematically considered and quantified. Periodic trends in gas-phase metal–hydride and metal–methyl bond energies, including prepublication citations of the results of this study, have been reviewed recently[2] and are discussed briefly here.

A very strong correlation exists between metal–hydride ion bond energies and metal ion promotion energies (E_P) for first-row metals. Here, E_P is defined as the energy needed to take the metal ion in its ground electronic state to an electronic configuration where there is one electron in the 4s orbital.[5,43,44] A similar but

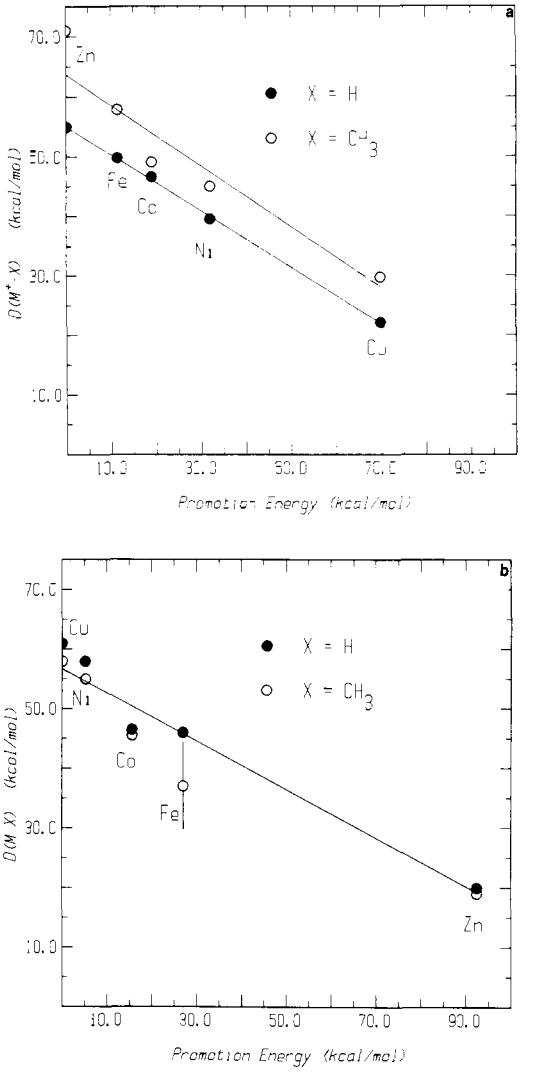

Figure 7. Ionic (a) and neutral (b) metal–methyl and metal–hydride bond dissociation energies vs atomic metal promotion energy. The solid lines show linear regression fits to the $M\text{–}H^+$, $M\text{–}CH_3^+$, and the average of M–H and $M\text{–}CH_3$ (excluding $FeCH_3$) bond energies.

not quite as good correlation emerges for bonding to the 3dσ orbital and for E_P vs metal–methyl ion bond energies. Neutral metal–hydride bond energies show good correlation with E_P[2,13] and with electron affinity.[13] Neutral metal–methyl bond energies parallel the metal–hydride bond energies exhibiting similar correlations with E_P. These general correlations are illustrated in Figure 7, which includes results for Fe and Zn for comparison. Note that for these five metals, the bond strengths for the ionic methyl species are stronger than the ionic metal hydrides by 8 ± 5 kcal/mol. The largest source of this difference is probably electrostatic in nature and therefore much more important for the more polarizable methyl ligand as compared with H. Indeed, Schilling et al.[45] estimate that this effect is worth ~5.5 kcal/mol. For the neutral species, where this effect is not important, the values for $D°(MH)$ are slightly stronger than $D°(MCH_3)$, by 3 ± 3 kcal/mol.

The strong correlation with promotion energy is consistent with a similar bonding picture for ionic and neutral metal–methyl and metal–hydride species, which primarily involves the metal 4s orbital, but can also include contributions from the 3dσ. This conclusion has been discussed previously for ionic species and is in agreement with ab initio calculations[38,45,46] for $M^+\text{–}H$ and

(41) Rappe, A. K.; Goddard, W. A. *J. Am. Chem. Soc.* **1977**, *99*, 3966–3968.
(42) Weil, D. A.; Wilkins, C. L. *J. Am. Chem. Soc.* **1985**, *107*, 7315–7320.
(43) Armentrout, P. B.; Halle, L. F.; Beauchamp, J. L. *J. Am. Chem. Soc.* **1981**, *103*, 6501–6502.
(44) Elkind, J. L.; Armentrout, P. B. *Inorg. Chem.* **1986**, *25*, 1078–1080. Elkind, J. L.; Armentrout, P. B. *J. Phys. Chem.* **1987**, *91*, 2037–2045.
(45) Schilling, J. B.; Goddard, W. A.; Beauchamp, J. L. *J. Am. Chem. Soc.* **1986**, *108*, 582–584; *Ibid.* **1987**, *109*, 5573–5580.

M^+–CH_3. Note that the correlation with E_P for MH^+ species is much better than that for MH or metal–methyl species. This may be partly due to the reduced accuracy in the latter thermochemistry. Another possibility is that the differences reflect somewhat different metal–ligand bonding. For neutral species, the deviations may reflect varying metal d or p orbital participation. For example, Bauschlicher et al.[38] find much less 3d orbital participation in the bonding of these neutral metal–methyls than in the ionic counterparts. For the metal–methyl species, there may be secondary interactions of metal d orbitals with other CH_3 orbitals, both vacant and occupied. In general, fully occupied CH_3 orbitals, especially the $CH_3(a_1)$, can cause destabilizing exchange repulsion interactions with occupied metal orbitals, while vacant $3d\pi$ orbitals can interact with the occupied $CH_3(e)$ orbitals to produce stabilizing (agostic) interactions.[47] This latter effect is expected only for early transition metals. No evidence for such agostic bonding is found in the ab initio calculations of Bauschlicher et al.[38] for ionic or neutral metal–methyls.

Let us now consider several isoelectronic species in the light of the available thermochemistry and general bonding framework that has been developed. The isoelectronic ZnH^+ and CuH have very strong bonds, 55 ± 3[48] and 61 ± 4 kcal/mol, respectively. Since Zn^+ and Cu both have an electronic configuration of $3d^{10}4s^1$, E_P is zero. Thus, the maximum bond energy can be expected, and indeed, these values are very close to the "intrinsic" metal–hydrogen bond energy for first-row transition metals (≃57 kcal/mol).[2,44] The ionic bond energy may be slightly weaker than the neutral because the charge on the metal center causes contraction of the metal bonding orbital which reduces bonding orbital overlap with the H(1s). This effect may also be related to the amount of 4p character that can mix with the 4s bonding orbital (less in the case of the ions).

For the analogous methyl ligands, $ZnCH_3^+$ (71 ± 3 kcal/mol)[14a] and $CuCH_3$ (58 ± 2 kcal/mol), the relative bond strengths are reversed. The $ZnCH_3^+$ bond is presumably stabilized by the electrostatic effect discussed above. The $ZnCH_3^+$ bond may be unusually strong compared to the other metal–methyl ions because Zn has a large ionization potential compared with the other metal ions (Table VII). Another important effect could be orbital contraction in the metal ion, which acts to stabilize M^+–CH_3 more than M^+–H. This is because reduced orbital overlap decreases exchange repulsion interactions between occupied metal orbitals and the fully occupied CH_3 orbitals. This effect finds no analogy for the H atom ligand.

The isoelectronic CuH^+ and NiH show very different bond strengths, 22 ± 3 and 58 ± 3 kcal/mol, respectively. This effect can be understood on the basis of the very different E_Ps (an effect that can also be traced to the charge-induced orbital contraction on the metal ions). Cu^+ forms weak bonds, since promotion of the very stable ground-state $3d^{10}$ configuration to a bonding configuration ($3d^94s^1$) is very costly, 70 kcal/mol.[44] Indeed, Bauschlicher et al.[38] find that when the metal retains the $3d^{10}$ configuration, the one-electron bond forms a low-lying electronic state of CuH^+ (and the ground state of $CuCH_3^+$). In contrast, the ground state of Ni is $3d^84s^2$, such that the promotion energy to $3d^94s^1$ is very low, 5 kcal/mol, allowing Ni to form strong bonds. The bond energies for the methyl species, $D°(CuCH_3^+)$ = 30 ± 2 and $D°(NiCH_3)$ = 55 ± 3 kcal/mol, parallel the hydride values, although the ionic metal–methyl is again somewhat stronger than the ionic hydride.

Discussion

The reaction mechanisms for the interactions of Co^+ and Ni^+ have been commented on extensively before.[4,7,17] The standard mechanism for such reactions is shown in Scheme I for the example of propane. Oxidative addition of a C–H or C–C bond

Scheme I

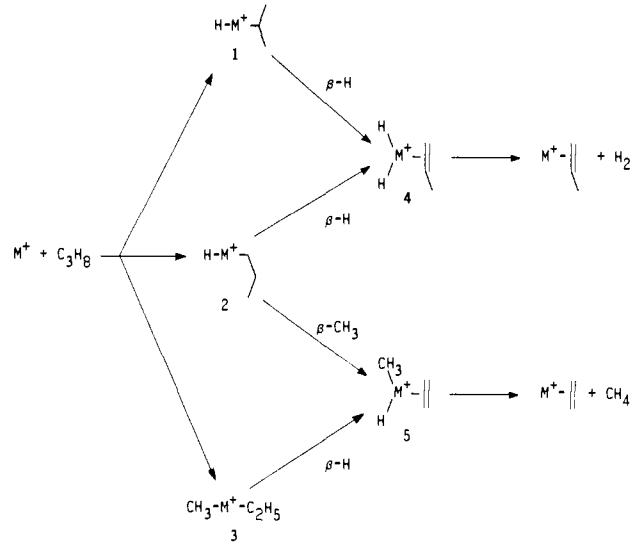

(M^+ insertion) forms intermediates **1**, **2**, or **3**. These rearrange by β-H or β-CH_3 shifts to the metal, followed by reductive elimination of H_2 from **4**, reaction 12, or of CH_4 from **5**, reaction 13. The other alkanes have similar reaction mechanisms. Our results are consistent with previous studies and with this mechanism. We therefore comment only on several features of these reactions that seem unusual in light of this mechanism.

Branching Ratios of Exothermic Channels. At low kinetic energies, Co^+ reacts exothermically with propane to eliminate more H_2 than CH_4, but as the energy is increased, this preference reverses such that methane elimination has the higher cross section (Figure 3a). This behavior is very unusual. Neither Ni^+ nor Fe^+[15] shows such behavior, and to our knowledge, it has not been observed in any other transition-metal system. Further, in the analogous reactions with isobutane, processes 15 and 16, Co^+ does not show a switch with kinetic energy (and neither does Ni^+ or Fe^+).[15]

The most obvious explanation for this behavior is that reaction 13 has a barrier. This would explain why the cross section for reaction 13 with Co^+ is much smaller and has a different shape than that with Ni^+, even though the cross sections for reaction 12 with Co^+ and Ni^+ have similar shapes and sizes. Indeed, the reaction cross section for reaction 12 shown in Figures 2a and 3a is entirely consistent (after convolution over the experimental energy distributions) with eq 7 when n = 0.5 and m = 1.0, the form predicted as the microscopic reverse of eq 6, σ_{LGS}.[49] The threshold that results is E_T = 0.025 ± 0.015 eV. After correcting for the electronic energy of Co^+ and including the error in the energy scale, we conclude that reaction 13 does not proceed until ground-state reactants have acquired 1.6 ± 0.7 kcal/mol of energy. This value is *not* the endothermicity of the reaction, however, since the overall reaction is exothermic by 26 ± 8 kcal/mol [$D°(Co^+$–$C_2H_4)$ = 46 ± 8 kcal/mol,[19] while the transformation $C_3H_8 \rightarrow C_2H_4 + CH_4$ requires only 19.6 kcal/mol]. Thus, the 1.6 kcal/mol barrier to the reaction must correspond to the transition state for the insertion step, the β-H or β-CH_3 migration step, or the CH_4 elimination step in Scheme I.

While it is difficult to assign a definitive mechanism, we think that a reasonable explanation is that there is a barrier in the last step of reaction 13, methane elimination from **5**, but no such barrier for reaction 12, H_2 loss from **4**. This is plausible since it has been calculated that CH_4 elimination from hydrido–metal–methyl species can have an activation barrier of ~30 kcal/mol, compared with small barriers (5–8 kcal/mol) for H_2 loss from the comparable metal–dihydride species[50] (although barriers may

(46) Pettersson, L. G. M.; Bauschlicher, C. W.; Langhoff, S. R.; Partridge, H. *J. Chem. Phys.* **1987**, *87*, 481–492.
(47) Ziegler, T.; Tschinke, V.; Becke, A. *J. Am. Chem. Soc.* **1987**, *109*, 1351–1358.
(48) Georgiadis, R.; Armentrout, P. B. *J. Phys. Chem.* **1988**, *92*, 7060–7067.
(49) Levine, R. D.; Bernstein, R. B. *J. Chem. Phys.* **1972**, *56*, 2281.
(50) Low, J. J.; Goddard, W. A. *J. Am. Chem. Soc.* **1984**, *106*, 6928, 8321; **1986**, *108*, 6115. Obara, S.; Kitaura, K.; Morokuma, K. *J. Am. Chem. Soc.* **1984**, *106*, 7482.

be smaller for ionic species due to the ion-induced dipole potential). For Co^+, we estimate that **5** and **4** in Scheme I are lower in energy than the reactants by 19 ± 8 and 7 ± 4 kcal/mol, respectively.[51] With the addition of the calculated barriers, these numbers suggest that the transition state for methane elimination could lie between 3 and 19 kcal/mol above the reactant energy while the transition state for dihydrogen elimination would lie 1 ± 5 kcal/mol *below* the reactant energy. These estimates are consistent with the experimental conclusion that there is an overall barrier for reaction 13 (of 1.6 ± 0.7 kcal/mol) compared with no barrier for reaction 12. Note, however, that the transition state for H_2 elimination is very close to the reactant energy, a conclusion that is consistent with the studies of Hanratty et al.[19] For ethane, the intermediate analogous to **5** is more stable than the reactants by only ≈4 kcal/mol, such that H_2 elimination should have a transition state *above* the reactant energy, consistent with the observed activation barrier for reaction 11. For larger alkanes, the intermediates analogous to **5** are more stable than **5** by only a couple of kilocalories per mole. However, even changes as small as this are sufficient to eliminate the 1.6 kcal/mol barrier observed for propane, such that these reactions show no overall barrier to methane elimination (Figures 4 and 5).

It still remains to explain why reaction 13 is *preferred* at higher energies if it is thermodynamically less favorable. This implies that this reaction is kinetically favored, i.e., formation of **5** occurs with higher probability than **4** at *all energies*. This, of course, is consistent with the observed behavior of Ni^+ and Fe^+. To try to understand these results, we refer to Scheme I where two limiting behaviors can be imagined. (1) Formation of intermediate **4** arises exclusively from C–H bond activation (via **1** or **2**), while formation of **5** occurs only via intermediate **3** (C–C bond activation). This presumes that β-alkyl transfers (required to form **5** from **2**) are inefficient, a conclusion that is not borne out by studies of larger alkanes.[17-20] In this limit of behavior, the branching ratio for reactions 12 and 13 will depend primarily on the ratio of C–H to C–C insertions. The results imply that the C–C insertion intermediate is formed preferentially, a result that can be justified on thermochemical grounds since Co^+–C bonds are stronger than Co^+–H bonds and the C–C bond is weaker than the C–H bond. (2) Both reactions occur exclusively via C–H bond insertion, where reaction 13 occurs via intermediate **2** while reaction 12 occurs via **1**. This requires that **2** *prefers* β-CH_3 transfer to β-H transfer, which can also be justified on thermochemical grounds since the Co^+–CH_3 bond is stronger than the Co^+–H bond and the C–C bond is weaker than the C–H bond. Now, the branching ratio will depend on the ratio of primary to secondary C–H bonds in propane, 3:1 in favor of reaction 13. Indeed, this has been forwarded as an explanation for why Fe^+ exhibits a 3:1 branching ratio for reactions 13 to 12, *independent* of the kinetic energy and electronic state.[15] This mechanism could be favored over the first mechanism due to steric factors, i.e., the C–H bonds are more accessible than the C–C bonds. Unfortunately, labeling studies cannot determine the insertion site, and it is clear that combinations of these behaviors could be involved.

For the case of Ni^+, reaction 13 is favored at all energies by a factor of 3.5–4.0. This has been justified on the basis of thermochemical estimates; C–C insertion is expected to be thermochemically favored while C–H insertion may be slightly endothermic for Ni^+. This is consistent with other work that indicates that Ni^+ preferentially inserts into the weakest C–C bond of linear alkanes.[18] There is no evidence of an overall reaction barrier in the case of Ni^+ reacting with any alkane studied here.

Reactivity of Cu^+. The endothermic reactions of Cu^+, a closed-shell $3d^{10}$ ion, are remarkably similar to the analogous reactions of Co^+ and Ni^+. This is in agreement with the findings of Elkind and Armentrout[16] that Co^+, Ni^+, and Cu^+ all have very similar reactivity with H_2. Further, Cu^+ reacts with H_2 at its thermodynamic limit, even though both Cu^+ and H_2 have closed shells. One difference in the reactivity of the three metal ions in the systems studied here is that formation of alkyl ions is much more strongly favored for Cu^+ reactions. This is because reactions 3 and 4 are accompanied by formation of the stable neutral copper species $CuH(^1\Sigma^+)$ and $CuCH_3(^1A_1)$ which have a pair of electrons in a σ-bonding orbital and a closed $3d^{10}$ shell on the metal.

Scheme II

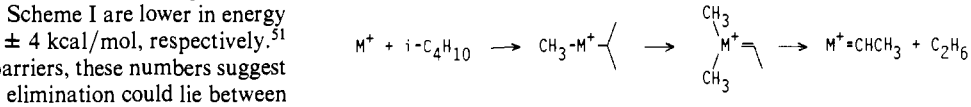

The most important difference between the reactivity of Cu^+ and other transition-metal ions is that Cu^+ does not react exothermically with alkanes. This can be attributed to the inability of Cu^+ to form intermediates **1**–**3** in Scheme I. Since Cu^+–H and Cu^+–CH_3 bonds are weak (Table VI), we estimate on the basis of bond additivity[51] that the full insertion of the copper ion into C–H and C–C bonds is endothermic by about 46 and 28 kcal/mol, respectively. This implies that C–H and C–C bond cleavage processes occur via a different mechanism.

The most plausible mechanism is *heterolytic* cleavage of the R–H and R–CH_3 bonds. This is naturally suggested by the dominance of reactions 3 and 4 over reactions 1 and 2. Further, this has been suggested as the mode of reaction for Pd^+ with alkanes.[52] Both Pd^+ and Cu^+ have hydride affinities (231 ± 6[52] and 221 ± 4 kcal/mol, respectively)[53] which are relatively high compared with most metal ions and just lower than that of the alkyl ions.[52] We imagine that the intermediates in these reactions involve a three-center two-electron bond, i.e., the two electrons in the C–H or C–C bond to be broken are donated into the empty 4s orbital of the Cu^+ ion. The formal cleavage of the C–H or C–C bond in this intermediate is probably not required and, indeed, is thermodynamically disfavored. When the energy is sufficiently high, this intermediate falls apart by alkyl ion loss, the lowest energy process available other than returning to reactants. The observation of long-lived adduct species in the isobutane and neopentane systems suggests that these intermediates are fairly stable species which do not readily decompose back to reactants. Indeed, Weisshaar and co-workers have observed that adduct formation between Cu^+ and C_3H_8 occurs at the LGS limit under flow tube conditions (0.75 Torr He).[32]

Formation of $NiC_2H_4^+$ and $CuC_2H_4^+$. One interesting species, observed in the reactions of Cu^+ and Ni^+ with isobutane, is $MC_2H_4^+$. This ion has also been observed in a study of Cu/isobutane cluster ions as a product from collision-induced dissociation of $Cu(C_4H_{10})_2^+$, but not $CuC_4H_{10}^+$.[54] These authors postulate an insertion of Cu^+ into each of the C–C bonds of the two isobutane molecules, but this is clearly not an option in the present study. We also note that $MC_2H_4^+$ is formed at anomalously high energies in the $Cu^+ + C_2H_6$ system (Figure 1c). In the $Ni^+ + C_2H_6$ system (Figure 1b), it is formed both at low energies (similar to Co^+) and at high energies (similar to Cu^+).

One possible explanation for this product is that it corresponds to the metal–ethylidene ion, $M^+{=}CHCH_3$. Since $CHCH_3$ ($\Delta_f H°$ = 88.5 kcal/mol)[55] is a much higher energy isomer than C_2H_4 ($\Delta_f H°$ = 12.5 kcal/mol), this would explain why it is only observed at high energies. Scheme II then provides a plausible mechanism for its formation from isobutane. This possibility can be evaluated by examining the thermodynamics of these reactions. For the Ni^+–isobutane system, the apparent threshold for $NiC_2H_4^+$ is 1.0–1.5 eV (23–35 kcal/mol) (Figure 4b). Since formation of C_2H_6 and $CHCH_3$ from isobutane requires 100.6 kcal/mol, this means that $D°(Ni^+{=}CHCH_3) \approx 66$–$78$ kcal/mol. This can be favorably compared with $D°(Ni^+{=}CH_2) = 76 \pm 3$ kcal/mol.[56]

(51) This assumes bond additivity, i.e., that the individual bond strengths do not change with the addition of more ligands. Within experimental error, this is in agreement with the estimate of Hanratty et al.[19] We also use their values for $D°(Co^+$–$C_2H_4)$ and $D°(Co^+$–$C_3H_6)$.[30]

(52) Tolbert, M. A.; Mandich, M. L.; Halle, L. F.; Beauchamp, J. L. *J. Am. Chem. Soc.* **1986**, *108*, 5675–5683.

(53) These are calculated from $D°(M^+$–$H^-) = D°(M$–$H) + IP(M) - EA(H)$ where EA(H) = 18.0 ± 0.5 kcal/mol.[37]

(54) Freas, R. B.; Campana, J. E. *J. Am. Chem. Soc.* **1985**, *107*, 6202–6204.

(55) Frenking, G.; Schmidt, J. *Tetrahedron* **1984**, *40*, 2123–2132.

Further, this figure would mean that $Ni^+{=}CHCH_3$ could be formed in the ethane system beginning about 1.4–1.8 eV, consistent with the high-energy reactivity observed in Figure 1b.

In the Cu^+–isobutane system, the apparent threshold for $CuC_2H_4^+$ is $\simeq$2.8 eV (65 kcal/mol) (Figure 4c), which suggests that $D°(Cu^+{-}CHCH_3) \approx 36$ kcal/mol. In the Cu^+–ethane system, the threshold for $CuC_2H_4^+$ is 3–4 eV (69–92 kcal/mol), which would mean that $D°(Cu^+{-}CHCH_3)$ is between 9 and 32 kcal/mol.

(56) Fisher, E. R.; Armentrout, P. B., work in progress. This value is somewhat lower than the generally accepted literature value of 86 ± 6 kcal/mol.[43]

Also, the observation of H_2 and D_2 loss in the $Cu^+ + CH_3CD_3$ system is consistent with formation of Cu^+–ethylidene. Since the $Cu^+(3d^{10})$ species cannot form a covalent double bond, it is possible that this is a dative interaction in which a singlet $CHCH_3$ donates its lone pair of electrons to the empty 4s orbital of Cu^+. This is consistent with the very weak bond energy derived.

Acknowledgment. We thank Nick Pugliano and R. H. Schultz for performing some of the Co^+ experiments. We would also like to thank C. W. Bauschlicher for communicating results prior to publication. This work was supported by National Science Foundation Grant No. CHE-8796289.

Copper Coordination in Nitrous Oxide Reductase from *Pseudomonas stutzeri*

Haiyong Jin,[†] Hans Thomann,[*,†,‡] Catherine L. Coyle,[*,†] and Walter G. Zumft[§]

Contribution from the Corporate Research Laboratory, Exxon Research and Engineering Company, Annandale, New Jersey 08801, and Lehrstuhl für Mikrobiologie, Universität Karlsruhe, Kaiserstrasse 12, D-7500 Karlsruhe 12, West Germany. *Received May 2, 1988*

Abstract: The structure of the copper sites in the multicopper enzyme nitrous oxide (N_2O) reductase from *Pseudomonas stutzeri* has been studied by electron paramagnetic resonance (EPR) and electron spin echo (ESE) spectroscopies. Correlations between the enzyme activity and paramagnetic susceptibility, the pH dependence of the EPR spectra, and exogenous ligand binding were investigated. Two types of copper sites are identified: antiferromagnetically coupled ($J > 200$ cm^{-1}) dimeric sites and unusual Cu(II) sites. The EPR susceptibility arises from these Cu(II) sites and from binuclear mixed-valence Cu(I)/Cu(II) half-met sites which may be derived from partially reduced dimers. On average, six of the eight copper ions per protein are in the form of the EPR-silent binuclear type 3 dimers. At $g = 2.03$ in the EPR spectrum, the Fourier transform of the stimulated echo envelope reveals a complex spectrum with narrow lines at 1.5, 1.9, 2.5, 2.9, and 3.4 MHz and broad lines centered at 0.8 and 3.8 MHz. This spectrum is not typical of either blue (type 1) or square-planar (type 2) sites in copper proteins. However, with the exception of the lines at 2.5 and 3.4 MHz, the spectrum for N_2O reductase is remarkably similar to that observed for the Cu_A site in cytochrome c oxidase. This is the first direct evidence that the Cu_A site exists in an enzyme other than cytochrome c oxidase. The ESE envelope spectrum can be simulated by using three sets of ^{14}N quadrupole coupling parameters. Two of these are characteristic of the distal nitrogen on imidazole ligands bound to Cu(II). By analogy to the ESE envelope spectra for the Cu_A site in cytochrome c oxidase, these two imidazole ligands are coordinated to the Cu_A site in N_2O reductase. The third ^{14}N, which is most likely coordinated to the half-met site, has a quadrupole coupling that is close to that observed by nuclear quadrupole resonance (NQR) spectroscopy for amide nitrogen and to that deduced from ESE measurements for the distal nitrogen of substituted imidazoles in copper–imidazole complexes. However, in both cases the quadrupole asymmetry is much smaller than that deduced from the present data. Water accessibility of the copper sites was investigated by ESE envelope spectroscopy. The deuteron modulation frequency observed for all forms of the enzyme dialyzed against D_2O at different pH values indicates that the EPR-active copper sites are accessible to water. A 10-fold increase in catalytic activity was observed after dialysis of the enzyme at pH 9.8. No concomitant change in the nitrogen ESE envelope spectrum was observed, but a significantly deeper deuteron modulation was observed for the enzyme dialyzed against D_2O. The envelope waveform is characteristic of a directly coordinated deuterated ligand, most likely a water or hydroxide. The increase in EPR line width and paramagnetic susceptibility, also observed at high pH, suggests that a new EPR-active copper site that has more exchangeable protons is generated at high pH. However, a pH-induced protein conformation change or base-catalyzed proton exchange allowing enhanced solvent accessibility to the copper sites cannot be ruled out.

Nitrous oxide (N_2O) is reduced to dinitrogen by denitrifying bacteria as part of the anaerobic respiration of nitrate to dinitrogen. Nitrous oxide reductase is the enzyme that catalyzes the reduction of N_2O to N_2 and H_2O. The multicopper enzyme from *Pseudomonas stutzeri* (formerly *Pseudomonas perfectomarina*) has been isolated and purified to homogeneity. The enzyme contains about eight copper atoms per molecular weight 140 000 and is composed of two identical subunits.[1] No other metal ions have been detected by plasma emission studies. Several different forms of the enzyme have been prepared. The more active purple form is obtained by purifying the enzyme under anaerobic conditions.[2] Aerobic purification of N_2O reductase produces a pink form that contains less copper and is 2–5-fold less active. Preparative isoelectric focusing of the purple form results in the resolution of two protein bands with slightly different isoelectric points (an anodic band at pI = 4.97 and a cathodic band at pI = 5.06). A blue inactive form is obtained by reduction with excess dithionite or ascorbate. A high-pH form of the enyzme, prepared by dialysis against buffer at pH 9.8, has an activity approximately 10-fold higher than that of the same enzyme at pH 7.5.[3]

Most copper centers in proteins have been classified into three types: "blue" (type 1), "normal" (type 2), and dimeric (type 3),

[†] Exxon Research and Engineering Company.
[*] Authors to whom correspondence should be addressed.
[‡] Also at Department of Chemistry, State University of New York, Stony Brook, Stony Brook, NY 11794.
[§] Universität Karlsruhe.

(1) Zumft, W. G.; Matsubara, T. *FEBS Lett.* **1982**, *148*, 107–112.
(2) Zumft, W. G.; Coyle, C. L.; Frunzke, K. *FEBS Lett.* **1985**, *183*, 240–244.
(3) Coyle, C. L.; Zumft, W. G.; Kroneck, P. M. H.; Korner, H.; Jakob, W. *Eur. J. Biochem.* **1985**, *153*, 459–467.

0002-7863/89/1511-4262$01.50/0